BJHH
BRAZILIAN JOURNAL OF HAIR HEALTH

CAECI
CENTRO DE APERFEIÇOAMENTO EDUCACIONAL E CIENTÍFICO

Original Research

Development and characterization of poly(lactic-co-glycolic acid) (PLGA) nanoparticles with finasteride and *in vivo* evaluation of their efficacy in hair growth

Lara Soares Junqueira [1, 2]; Mariana Sato de Souza de Bustamante Monteiro [3], Lucio Mendes Cabral [2, *]

[1] Graduate Program in Pharmaceutical Sciences. Federal University of Rio de Janeiro, Faculty of Pharmacy, Rio de Janeiro, Brazil.
[2] Industrial Pharmaceutical Technology Laboratory. Federal University of Rio de Janeiro, Faculty of Pharmacy, Rio de Janeiro, Brazil.
[3] Galenic Development Laboratory. Federal University of Rio de Janeiro, Faculty of Pharmacy, Rio de Janeiro, Brazil.

***** Correspondence: larasjunqueira@gmail.com.

Abstract

Introduction: Alopecia is a condition that affects the hair follicle, characterized by hair loss, with multifactorial etiology. This disorder often impacts the social and psychological well-being of the individual. Currently, a wide variety of treatments are available, including topical, oral, injectable formulations, and hair transplantation. Oral therapies are the most adhered to; however, they generally present more adverse effects. As a well-established oral drug therapy, finasteride is presented, which inhibits the enzyme 5-α-reductase, and blocks the conversion of testosterone into dihydrotestosterone (DHT). This drug is capable of promoting hair growth, however, it needs to be used over long periods, which can lead to adverse effects. Therefore, in this work, poly(lactic-co-glycolic acid) (PLGA) nanoparticles with finasteride were developed, aiming to improve the efficiency of this drug and reduce its systemic side effects.

Methodology: Nanoparticles without the drug and with the drug at concentrations of 10 mg, 20 mg, and 30 mg were developed. The system was characterized by Dynamic Light Scattering (DLS), Zeta Potential, Differential Scanning Calorimetry (DSC), and Fourier Transform Infrared Spectroscopy (FTIR) techniques.

Results and Conclusion: The drug-free nanoparticles had a reaction yield of 91.8 ± 3.9%, nanoparticles with 10 mg of finasteride showed a yield of 82.6 ± 7.8%, with 20 mg a yield of 92.9 ± 3.7%, and with 30 mg a yield of 89.3 ± 1.0%. The average diameter ranged from 162.2 ± 8.2 nm for drug-free nanoparticles, 176.1 ± 0.7 nm for nanoparticles with 10 mg of finasteride, 179.6 ± 3.3 nm for nanoparticles with 20 mg, and 187.7 ± 4.5 nm for nanoparticles with 30 mg. Nanoparticles with 10 mg of finasteride showed an encapsulation efficiency of 48.2 ± 30%, nanoparticles with 20 mg an efficiency of 90.7 ± 9.9%, and nanoparticles with 30 mg an efficiency of 83.2 ± 23.5%. The development of nanoparticles and the encapsulation of finasteride were successful. Next, an in vivo study will be conducted to evaluate its efficacy in promoting hair growth orally in Wistar rats.

Keywords: PLGA Nanoparticles; Finasteride; Alopecia; Hair Growth; Hair Loss.

Citation: Junqueira LS, Monteiro MSSB, Cabral LM. Development and characterization of poly(lactico-glycolic acid) (PLGA) nanoparticles with finasteride and in vivo evaluation of their efficacy in hair growth. Brazilian Journal of Hair Health. 2024; 1:bjhh13.

doi: https://doi.org/10.62742/2965-7911.2024.1.bjhh13

Received: May 18, 2024
Revised: May 18, 2024
Accepted: May 18, 2024
Published: May 18, 2024

1. Introduction

Alopecia is a condition affecting the hair follicle, characterized by hair loss. Moreover, it is a chronic inflammatory disease with multifactorial etiology, including metabolic and

autoimmune disorders [1]. Its incidence increases with age, affecting about 80% of men by the age of 70 [2]. In women, the prevalence is around 56% at 75 years [3]. The most common type of hair loss is androgenetic alopecia (AGA), also known as male pattern baldness. It is a condition with a high prevalence, where 80% will show symptoms by the age of 70 [4]. Its most common characteristic is the progressive miniaturization of the hair follicle, which leads to a gradual decrease in the anagen phase and an increase in the telogen phase. The advancement of the disease promotes an increasingly reduced hair cycle that results in thinner and shorter hair [2]. The main mechanisms involved in the pathophysiology of AGA include genetic predisposition, androgen metabolism, and microinflammation in the scalp region [5]. Androgens play a significant role in this pathology, as their action regulates the production of cytokines and growth factors in the dermal papillae, important factors for maintaining the anagen phase [6]. Moreover, hair follicles express androgen receptors, which dihydrotestosterone (DHT) acts upon and induces early hair regression, hair miniaturization, and morphological changes [7].

The treatment of AGA involves a multimodal clinical management due to its complex pathophysiology. However, there are only two drug therapies approved by the Food and Drug Administration (FDA) for the treatment of this condition. They are oral finasteride and topical minoxidil [8]. This study will focus on finasteride, which will be the model drug used in the developed system.

Finasteride, a synthetic 4-azasteroid compound, is a specific and competitive inhibitor of type II 5α-reductase. It is an effective strategy in the treatment of male hair loss, given the increased expression of androgen receptors and DHT in the hair follicles of the bald area [9]. Finasteride inhibition prevents the conversion of testosterone into DHT in the skin, liver, and prostate [10]. Androgens affect hair growth as important regulators, which can stimulate, leave unchanged, or inhibit terminal hair growth depending on the body region. In the scalp follicles, androgens can impair hair growth, promote miniaturization, and reduce the anagen phase, which are the classic symptoms of baldness [4]. Moreover, there is evidence in the literature that DHT converts terminal hairs into miniaturized hairs, leading to gradual hair loss. Therefore, DHT suppression induced by finasteride can promote hair growth [11].

However, the use of finasteride in cases of AGA in men has resulted in the use of this medication by younger patients and for a longer period due to its drug-dependent nature. When the administration of the drug is stopped, hair loss recurs. Thus, a significant obstacle to the use of finasteride is patient resistance related to its adverse effects. Among the most severe adverse effects are sexual and reproductive effects, where the use of 1 mg/day, the approximate dose indicated for alopecia, can cause erectile dysfunction, although not permanently. Among the reproductive effects is fertility, which may be affected by the use of this medication [12].

One strategy to improve the efficiency of drug delivery to a target site and significantly reduce adverse effects, such as those of finasteride, involves the use of nanotechnology [13]. In this sense, nanometric systems have gained attention for being able to contribute to the accumulation of therapeutic agents in hair follicles and increase the efficiency in treating alopecia [14]. Formulating a drug vehicle, such as finasteride, in a nanosystem can provide effective administration and reduce adverse effects. This is possible because a drug incorporated into a nanoparticle allows its stabilization in environments such as the gastrointestinal tract, can increase its solubility and bioavailability, and provide more efficient release at specific action sites [15]. Thus, nanoparticles (NPs) offer targeted therapy compared to conventional therapies [16].

Moreover, one of the main challenges of oral drug administration is its ability to overcome multiple compartments, such as stomach pH, and have good absorption by enterocytes in the small intestine to reach the bloodstream with bioavailability and be capable of producing a therapeutic effect. In this sense, nanomaterials are capable of protecting active ingredients from adverse stomach and intestine conditions; increase intestinal absorption into the bloodstream; reach specific human body cells; and ensure modified release within a target cell of interest [17]. Thus, polymeric NPs are excellent drug delivery systems for oral administration, as they are biocompatible, biodegradable, non-toxic, and safe for human use. They also have good stability and are capable of encapsulating large amounts of active ingredients [15]. They are also capable of promoting targeted and modified drug release and improving their therapeutic indices [18]. For their development, synthetic biodegradable polymers such as polyesters, poly (glycolic acid) (PGA), poly (D-L-lactic acid) (PLA), and poly-lactic-co-glycolic acid (PLGA) are used. These materials are advantageous as they exhibit less variability

and immunogenicity between batches compared to biodegradable polymers from natural sources [18].

PLGA is the most used biodegradable polymer in drug delivery systems due to its long history of clinical use, favorable behavior, and degradation. It is also capable of incorporating a variety of therapeutic agents [18]. It exhibits an enhanced permeability and retention (EPR) effect; this passive targeting of NPs is based on their properties, such as size, shape, and surface charge, which allows them to accumulate in a specific microenvironment, as seen in cancer cells [16]. It is a promising material for drug encapsulation, notably finasteride, since this active ingredient has a high encapsulation efficiency with PLGA, indicating a high interaction between these compounds due to the high degree of lipophilicity of finasteride [19]. This is an efficient way to enhance the bioavailability of this drug, which in turn does not have a long-lasting therapeutic effect due to its low water solubility [20].

To date, only nanosystems with finasteride for topical application are described in the literature. However, topical application of finasteride does not result in significant systemic absorption. The lack of effect of finasteride through this route of application suggests that oral finasteride is a more effective option, as it reduces circulating levels of DHT more efficiently [21]. The development of polymeric finasteride NPs for topical use exhibited in vitro release assay a prolonged release of 3 hours and in the in vitro skin permeation assay presented low penetration levels, showing a longer stay on the skin [22]. Topically applied drugs must have a level of permeation that allows them to cross the superficial layers of the skin but remain retained in the epidermis and exert only a local effect [23].

The systemic application of finasteride NPs was evaluated in a study that developed polymeric microspheres containing this drug and tested in AGA. However, it was used subcutaneously. The results were promising, as the administration of NPs promoted hair growth in 86.7% of the mice, and serum levels of DHT decreased after 6 weeks of treatment. Additionally, they exhibited follicular length, anagen/telogen phase ratio, and hair bulb diameter values like the group treated with oral finasteride [24]. Despite the good results at a systemic level, the subcutaneous route does not have a high adherence and acceptance rate by the public [25]. So far, there are no studies indicating the effects of NPs at a systemic level, orally, and how it behaves passing through different barriers of the digestive system. Therefore, the current study aims to develop and characterize PLGA NPs with finasteride and test their efficacy in vivo through oral administration.

2. Methodology

2.1 Development of PLGA nanoparticles

The synthesis of the PLGA nanoparticle initially involved developing an aqueous phase. In this step, 110 mg of Lutrol was dissolved in 30 mL of distilled water and subjected to magnetic stirring until solubilization. Then, the organic phase was composed of 110 mg of PLGA dissolved in 7 mL of acetone, under magnetic stirring. Once both phases were solubilized, a Pasteur pipette was used to drip the organic phase into the aqueous phase. The system was then stirred for 5 minutes at room temperature. For complete extraction of the organic solvent, the NPs were subjected to a rotary evaporator for 30 minutes.

2.2 Development of PLGA nanoparticles with finasteride

The development of PLGA NPs with finasteride followed the same procedure described in Item 2.1. However, 10 mg, 20 mg, or 30 mg of the active ingredient were added to the organic phase and solubilized under magnetic stirring. The different drug concentrations were used to evaluate the best encapsulation efficiency. After solubilization, the PLGA was added and followed the standard process mentioned previously.

Finally, the NPs were lyophilized for 72 hours for further characterization. Dynamic Light Scattering (DLS) and Zeta Potential analyses were conducted on the suspensions after nanoparticle synthesis.

2.3 Calculation of the yield of the nanoparticle development process

The weight of the nanoparticle after the lyophilization process was compared with its initial mass, in order to calculate the yield of this process, using the following equation:

Yield (%) = Weight of the nanoparticle after lyophilization x 100 / (Weight of Polymer + Weight of Surfactant + Weight of Active Ingredient)

2.4 Characterization of nanoparticles

The characterization of the NPs was performed using the following techniques: Dynamic Light Scattering (DLS), Zeta Potential, Differential Scanning Calorimetry (DSC), Fourier Transform Infrared Spectroscopy (FTIR), and Encapsulation Efficiency.

2.4.1 Dynamic light scattering (DLS)

This analysis was performed to assess the average diameter and polydispersity index of the NPs. This measurement was obtained using a ZetaPALS-31448 analyzer (Holtsville, New York), using a 1 cm optical path quartz cuvette, with a detection angle of 90°, a refractive index of 1.33, and temperature of 25 °C. All measurements were performed in triplicate. The nanosystems after synthesis were diluted in a 1:20 [v/v] ratio with distilled water for reading in the device. Simultaneously, particle size analysis was obtained to evaluate the homogeneity of the nanosystem in suspension.

2.4.2 Zeta potential

The Zeta Potential was conducted to obtain the surface charge of the NPs. To determine the charge, they were evaluated in a ZetaPALS-31448 analyzer, Brookhaven Instruments (Holtsville, USA), at room temperature (25 °C). The same dilution used in Item 2.4.1 was performed. The reading took place in a standard polystyrene cuvette (1 cm) and a parallel plate electrode (0.45 cm2 platinum plates with a 0.4 cm gap) was inserted. All analyses were done in triplicate.

2.4.3 Differential scanning calorimetry (DSC)

Thermal analysis of the nanoparticles was performed using a Shimadzu DSC-60 differential scanning calorimeter (Tokyo, Japan). About 1 mg of sample was placed and sealed in an aluminum pan and then subjected to a heating rate of 10°C min-1 in a temperature range from 30°C to 300°C, under an inert nitrogen gas environment at a flow rate of 50 mL/min. An empty aluminum pan was used as a reference.

2.4.4 Fourier transform infrared spectroscopy (FTIR)

The FTIR patterns of the samples were obtained in the range between 400 and 4000 cm-1 using a SHIMADZU IR PRESTIGE-21 Fourier transform infrared absorption spectrometer (Tokyo, Japan). The samples were prepared by forming pellets with 1% [w/w] of previously dried and powdered potassium bromide (KBr).

2.4.5 Encapsulation efficiency

The encapsulation efficiency (EE%) of the NPs was estimated from the percent difference between the drug concentration in the mother solution and the concentration present in the particles. To evaluate the encapsulation efficiency of finasteride in the NPs, a mother solution of 100 µg/ml finasteride with dichloromethane was developed. Subsequently, a serial dilution of 5 µg/ml, 10 µg/ml, 15 µg/ml, 20 µg/ml, and 25 µg/ml was performed. Afterwards, solutions with the NPs incorporating 10 mg, 20 mg, and 30 mg of finasteride were made. The aliquots from the mother solution and each solution were analyzed at the wavelength (λ) 254 nm on a UV/VIS Spectrophotometer, model V-630, Jasco. All analyses were performed in triplicate.

3. Results

3.1 Calculation of reaction yield for nanoparticle development

The yield calculations for the NPs without drug and with finasteride 10 mg, 20 mg, and 30 mg are represented in Table 1. In the development of the NPs, the average reaction yield was 89.1 ± 4.0%.

Table 1. Result of the reaction yield of the nanoparticles. The left column represents the samples, and the right column shows the values of the average yields in percentage and their standard deviation.

Sample	Yield (%)
PLGA-Blank	91.8 ± 3.9
PLGA-F10mg	82.6 ± 7.8
PLGA-F20mg	92.9 ± 3.7
PLGA-F30mg	89.3 ± 1.0

All measurements were conducted in triplicate, represented by the mean and standard deviation.

The drug-free NPs had a yield of 91.8 ± 3.9%, the NPs with 10 mg of finasteride had a yield of 82.6 ± 7.8%, the NPs with 20 mg of finasteride had a yield of 92.9 ± 3.7%, and the NPs with 30 mg of finasteride had a yield of 89.3 ± 1.0%.

3.2 Characterization of nanoparticles

3.2.1 Determination of average diameter and polydispersity index of nanoparticles

The average diameter and polydispersity index of the NPs are found in Table 2. The nanoparticle without active ingredient showed an average diameter of 162.2 ± 8.2 nm, the nanoparticle with 10 mg of the active ingredient exhibited an average diameter of 176.1 ± 0.7 nm, the nanoparticle with 20 mg showed an average diameter of 179.6 ± 3.3 nm, and the nanoparticle with 30 mg of finasteride presented an average size of 187.7 ± 4.5 nm.

Table 2. Average Diameter and Polydispersity Index of the nanoparticles. The left column represents the name of the samples, the middle column the average diameter of the nanoparticles in nanometers, and the right column the polydispersity index.

Sample	Average Diameter (nm)	Polydispersity Index (PdI)
PLGA-Blank	162.2 ± 8.2	0.1 ± 0
PLGA-F10mg	176.1 ± 0.7	0.1 ± 0
PLGA-F20mg	179.6 ± 3.3	0.1 ± 0
PLGA-F30mg	187.7 ± 4.5	0.2 ± 0

All measurements were conducted in triplicate, represented by the mean and standard deviation.

This analysis also evaluated the Polydispersity Index (PdI) of the nanoparticles. The PdI of the nanoparticles was predominantly 0.1 ± 0, except for the nanoparticle with 30 mg of the drug, which exhibited a PdI of 0.2 ± 0. The values were close to 0, indicating a high homogeneity in the distribution of the nanoparticles and the presence of only one population.

3.2.2 Determination of zeta potential of nanoparticles

From the zeta potential, it is possible to determine the effective surface charge of the particle, such measurement is related to the stability of the suspension and the morphology of the particle surface. Zeta potential values are not an absolute measure of nanoparticle stability, but they are indicative (Samimi, et al., 2019). Table 3 presents the zeta potential and pH of the nanoparticles.

Table 3. Zeta Potential and pH of the nanoparticles. The left column represents the name of the samples, the middle column the pH value, and the right column the zeta potential.

Sample	pH	Zeta Potential (mV)
PLGA-Blank	5	-25.2 ± 0.7
PLGA-F10mg	5	-21.1 ± 2.9
PLGA-F20mg	5	-18.6 ± 1.5
PLGA-F30mg	5	-14.8 ± 2.5

All measurements were conducted in triplicate, represented by the mean and standard deviation.

The drug-free nanoparticles showed negative zeta potential values of -25.2 ± 0.7 mV. This result is consistent with the literature, where PLGA NPs exhibit zeta potential variations between -26.8 mV and -30.0 mV (Hernández-Giottonini, et al., 2020). The incorporation of finasteride increased the zeta potential, where the NPs with 10 mg of finasteride displayed values of -21.1 ± 2.9 mV, the nanoparticles with 20 mg -18.6 ± 1.5 mV, and -14.8 ± 2.5 mV for the system with 30 mg of the drug.

3.2.3 Determination of differential scanning calorimetry (dsc) of the nanoparticles

The DSC thermogram of finasteride showed an endothermic event, with a characteristic peak at 259.3 °C (Table 4), which corresponds to the melting point of finasteride (Ahmed, 2016).

Table 4. DSC Analysis of the nanoparticles. The left column represents the name of the samples, and the right column represents the endothermic events of the respective samples and their values in °C.

Sample	Endothermic Event (°C)
Finasteride	259.3
PLGA-Blank	55.6
PLGA-F10mg	53.1
PLGA-F20mg	53.2
PLGA-F30mg	55.3

The PLGA nanoparticle without drug incorporation showed an endothermic event at 55.6 °C related to the glass transition of the polymer (De Souza Furtado, et al., 2023). The nanoparticles incorporated with finasteride exhibited 53.1°C, 53.2°C, and 55.2°C for the addition of 10 mg, 20 mg, and 30 mg of the drug, respectively.

3.2.4 Determination of fourier transform infrared spectroscopy (FTIR) of the nanoparticles

Figure 1 shows the spectra of finasteride, the nanoparticle without active incorporation, and the NPs containing different concentrations of finasteride, namely 10 mg, 20 mg, and 30 mg. In the drug-free NPs, the absorption bands of PLGA at 2919 cm^-1 represent the methylene group, the carbonyl group at 1758 cm^-1, and the ester group at 1172 cm^-1 and 1094 cm^-1 (De Souza Furtado, et al., 2023). Finasteride analysis showed characteristic peaks at 3428, 1668, and 1598 cm^-1, corresponding to the amide grouping, and other peaks at 1395-1383/1365 cm^-1 representing three functional groups: amide, ketone, and alkyl groups. The peak at 2966 cm^-1 represents a methyl group and 1668 cm^-1 the carbonyl group (Ahmed, 2016). The nanoparticles encapsulated with finasteride at concentrations of 10 mg, 20 mg, and 30 mg showed a shift and loss of intensity of the 1758 cm^-1 peak (carbonyl group) of PLGA to 1463 cm^-1. The ester group of PLGA also shifted and lost intensity to 1053 cm^-1. The 2919 cm^-1 band of the methylene group shifted to 2620 cm^-1. The peak of finasteride at 1365 cm^-1 lost intensity.

3.2.5 Encapsulation efficiency of nanoparticles incorporated with finasteride

For the encapsulation efficiency (EE%) of finasteride, an adaptation of the protocol by Vijaya Lakshmi (2013) was used, which is a method for quantifying finasteride by UV/VIS spectrophotometry. From the absorbance values measured in solutions with different concentrations of finasteride incorporated into the nanoparticle, it was possible to calculate the percentage of finasteride in that system. This data is presented in Table 5.

The nanoparticle with 10 mg of finasteride showed an encapsulation degree of 48.2 ± 30%. The NPs with higher concentrations of finasteride, 20 mg and 30 mg, showed encapsulation efficiency percentages of 90.7 ± 9.9% and 83.2 ± 23.5%, respectively. The nanoparticle that exhibited the best encapsulation efficiency and will be used for the in vivo study is the nanoparticle with 20 mg of finasteride.

Figure 1. FTIR Spectrum of PLGA nanoparticles without active incorporation, with finasteride incorporation at different concentrations, and the model drug (finasteride). The x-axis represents the wavelength, and the y-axis represents the transmittance of the analyzed samples: blank nanoparticle (black), nanoparticle with 10 mg of finasteride (red), nanoparticle with 20 mg of finasteride (blue), nanoparticle with 30 mg of finasteride (green), and finasteride (purple).

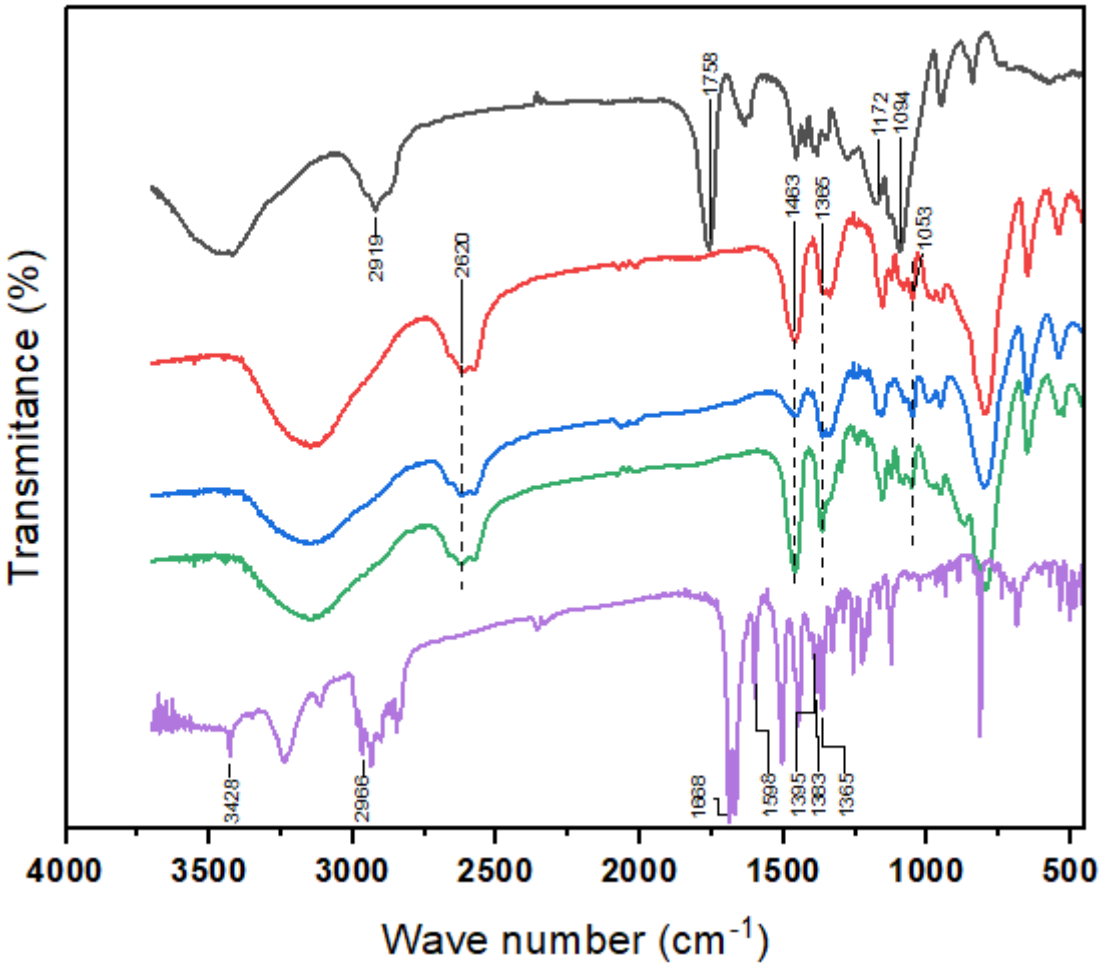

Table 5. Percentage of finasteride concentration incorporated by the nanoparticles. The left column is the name of the samples, and the right column represents the percentage of finasteride incorporated into the nanoparticles with 10 mg, 20 mg, and 30 mg of finasteride.

Sample	Finasteride Concentration (%)
PLGA-F10mg	48.2 ± 30
PLGA-F20mg	90.7 ± 9.9
PLGA-F30mg	83.2 ± 23.5

All measurements were performed in triplicate, represented by the mean and standard deviation.

4. Discussion

The present study aimed to develop finasteride-encapsulated NPs to enhance the efficacy of this drug in promoting hair growth. The results suggest that the synthesis of NPs was successful using the proposed methodology. The NPs exhibited a high reaction yield, with an average of 89.1 ± 4.0%, indicating satisfactory yield. This high yield could be attributed to the absence of filtration or centrifugation after their synthesis. Motawea et al. [26] also described a high reaction yield of PLGA nanoparticles developed with the surfactant lutrol, ranging from 71.64 ± 7.49% to 88.93 ± 5.76%. Additionally, the average size was 162.2 ± 8.2 nm for NPs without the drug, 176.1 ± 0.7 nm for NPs with 10 mg of finasteride, 179.6 ± 3.3 nm for NPs with 20 mg, and 187.7 ± 4.5 nm for NPs with 30 mg. This indicates that increasing the addition

of the drug during NP synthesis correlated with an increase in NP size, especially for NPs with 20 mg and 30 mg of finasteride. These results are consistent with literature findings, where values of 178.50 ± 10.30 nm were obtained for this nanoparticle model [27]. The NPs without the drug exhibited negative zeta potential values of -25.2 ± 0.7 mV, consistent with the presence of PLGA, a negatively charged polymer [27]. This phenomenon can be explained by the terminal carboxylic acid groups present in the copolymer [28].

This size range along with the negative charge is promising for oral application, as anionic NPs with diameters smaller than 200 nm induce relaxation of tight junctions between enterocytes, resulting in increased intestinal permeability [29]. Moreover, negative zeta potential values are associated with higher kinetic stability and lower cytotoxicity levels [16]. The incorporation of finasteride increased the zeta potential, reaching -14.8 ± 2.5 mV for the system with 30 mg of drug. This suggests the presence of finasteride adsorbed on the surface of the NPs, resulting in a slight neutralization of the negative charge of PLGA, corresponding to the presence of carboxylic terminal groups, leading to a reduction in zeta potential compared to drug-free NPs [22].

The DSC and FTIR results supported the hypothesis that the NPs were successfully synthesized. The melting point of the drug was not present in the DSC curves of NPs with finasteride, indicating the absence of crystalline drugs in the NPs and suggesting that the encapsulated drug underwent amorphization and loss of crystallinity due to its molecular dispersion in the polymeric matrix of the NPs [30]. The addition of 10 mg and 20 mg of finasteride showed a slight reduction in the endothermic event, suggesting that the drug overlaid the glass transition temperature of PLGA, indicating a reduction in attractive forces between polymer chains, leading to a slight reduction in the polymer's thermal profile [31]. Generally, encapsulating active ingredients in PLGA nanoparticles results in a displacement and loss of intensity in the characteristic peaks of this polymer in the FTIR technique [32]. The absence of characteristic peaks of finasteride when incorporated into NPs in the FTIR analysis may indicate encapsulation of the drug in the core rather than surface binding [26]. The NP with 10 mg of finasteride showed a low encapsulation degree of 48.2 ± 30%, suggesting that the low drug concentration may not achieve satisfactory encapsulation efficiency. However, higher concentrations of finasteride, with 20 mg and 30 mg, showed higher encapsulation efficiency percentages, being 90.7 ± 9.9% and 83.2 ± 23.5%, respectively.

The high encapsulation efficiency can be explained by the synthesis method used for the nanoparticles. The nanoprecipitation method allows for high solubilization of a hydrophobic drug like finasteride in an organic solvent, as acetone was used to incorporate the active ingredient into the polymeric matrix. Additionally, high encapsulation efficiency values (79.49 ± 0.47%) have been previously described for PLGA nanoparticles incorporated with finasteride [22]. Highly hydrophobic drugs like finasteride have an affinity with PLGA, leading to high encapsulation efficiency. On the other hand, the high lipophilicity of PLGA results in interpenetration with the hydrophobic fractions of lutrol, forming interconnected networks around nanoparticles loaded with the active ingredient, increasing the encapsulation efficiency of finasteride within the core [26].

The next step of the study will involve the oral administration of finasteride-encapsulated nanoparticles, controlled by placebo and conventional finasteride administration in rats.

5. Conclusion

The nanoprecipitation method for NP synthesis was successful, yielding satisfactory results and high drug encapsulation efficiency. Additionally, the NPs exhibited an appropriate average size range and a negative charge, which may promote greater intestinal permeability and enhanced biodistribution efficacy. Therefore, the results thus far indicate a nanosystem with promising characteristics for oral administration. The next step of the study will be to test the efficacy and safety of the nanoparticles in promoting hair growth in vivo.

Funding: None.

Institutional Review Board Statement and/or Informed Consent Statement: None.

Acknowledgments: None.

Conflicts of Interest: The authors declare no conflicts of interest.

References

1. Ablon G, Kogan S. A randomized, double blind, placebo controlled study of a nutraceutical supplement for promoting hair growth in perimenopausal, menopausal, and postmenopausal women with thinning hair. 2021.
2. Nestor MS, et al. Treatment options for androgenetic alopecia: Efficacy, side effects, compliance, financial considerations, and ethics. J Cosmet Dermatol. 2021;20(12):3759-3781.
3. Starace M, et al. Female androgenetic alopecia: an update on diagnosis and management. Am J Clin Dermatol. 2020;21:69-84.
4. Lolli F, et al. Androgenetic alopecia: a review. Endocrine. 2017;57:9-17.
5. Katzer T, et al. Physiopathology and current treatments of androgenetic alopecia: Going beyond androgens and anti-androgens. Dermatol Ther. 2019;32(5):e13059.
6. Rossi A, et al. Multi-therapies in androgenetic alopecia: Review and clinical experiences. Dermatol Ther. 2016;29(6):424-432.
7. Fu D, et al. Dihydrotestosterone-induced hair regrowth inhibition by activating androgen receptor in C57BL6 mice simulates androgenetic alopecia. Biomed Pharmacother. 2021;137:111247.
8. Devjani S, et al. Androgenetic alopecia: therapy update. Drugs. 2023;83(8):701-715.
9. Haber RS. Pharmacologic management of pattern hair loss. Facial Plast Surg Clin North Am. 2004;12(2):181-189.
10. Iamsumang W, Leerunyakul K, Suchonwanit P. Finasteride and its potential for the treatment of female pattern hair loss: evidence to date. Drug Des Devel Ther. 2020;14:951-959.
11. Gupta AK, Talukder M. Topical finasteride for male and female pattern hair loss: Is it a safe and effective alternative?. J Cosmet Dermatol. 2022;21(5):1841-1848.
12. Carreño-Orellana N, et al. Efectos adversos de finasteride: mitos y realidades. Una revisión actualizada. Rev Med Chil. 2016;144(12):1584-1590.
13. Patra JK, et al. Nano based drug delivery systems: recent developments and future prospects. J Nanobiotechnology. 2018;16(1):1-33.
14. Vidlářová L, et al. Nanocrystals for dermal penetration enhancement—Effect of concentration and underlying mechanisms using curcumin as model. Eur J Pharm Biopharm. 2016;104:216-225.
15. Date AA, Hanes J, Ensign LM. Nanoparticles for oral delivery: Design, evaluation and state-of-the-art. J Control Release. 2016;240:504-526.
16. Chiu HI, et al. Cytotoxicity of targeted PLGA nanoparticles: A systematic review. RSC Advances. 2021;11(16):9433-9449.
17. Reinholz J, Landfester K, Mailänder V. The challenges of oral drug delivery via nanocarriers. Drug Deliv. 2018;25(1):1694-1705.
18. Kamaly N, et al. Degradable controlled release polymers and polymeric nanoparticles: mechanisms of controlling drug release. Chem Rev. 2016;116(4):2602-2663.
19. Sahu P, Ramteke H. Biomaterials for Treatment of Baldness. Cureus. 2022;14(11).
20. Soleymani SM, Salimi A. Enhancement of dermal delivery of finasteride using microemulsion systems. Adv Pharm Bull. 2019;9(4):584.
21. Price TM, Allen S, Pegram GV. Lack of effect of topical finasteride suggests an endocrine role for dihydrotestosterone. Fertil Steril. 2000;74(2):414-415.
22. Roque LV, et al. Design of finasteride-loaded nanoparticles for potential treatment of alopecia. Skin Pharmacol Physiol. 2017;30(4):197-204.
23. Gomes MJ, et al. Lipid nanoparticles for topical and transdermal application for alopecia treatment: development, physicochemical characterization, and in vitro release and penetration studies. Int J Nanomedicine. 2014;9:1231-1242.
24. Kim JH, et al. Development of finasteride polymer microspheres for systemic application in androgenic alopecia. Int J Mol Med. 2019;43(6):2409-2419.
25. Ridyard CH, et al. A systematic review of patients' perspectives on the subcutaneous route of medication administration. Patient. 2016;9:281-292.
26. Motawea A, et al. Crucial role of PLGA nanoparticles in mitigating the amiodarone induced pulmonary toxicity. Int J Nanomedicine. 2021;16:4713-4737.
27. Machado ME, et al. Novel rivaroxaban loaded poly (lactic co glycolic acid)/poloxamer nanoparticles: Preparation, physicochemical characterization, in vitro evaluation of time dependent anticoagulant activity and toxicological profile. Nanotechnology. 2021;32(13):135101.
28. Rezaei G, et al. Synthetic and biological identities of polymeric nanoparticles influencing the cellular delivery: an immunological link. J Colloid Interface Sci. 2019;556:476-491.
29. Lamson NG, et al. Anionic nanoparticles enable the oral delivery of proteins by enhancing intestinal permeability. Nat Biomed Eng. 2020;4(1):84-96.
30. Ghasemian E, et al. Preparation, characterization and optimization of sildenafil citrate loaded PLGA nanoparticles by statistical factorial design. DARU J Pharm Sci. 2013;21:1-10.
31. Sánchez-López E, et al. Dexibuprofen biodegradable nanoparticles: One step closer towards a better ocular interaction study. Nanomaterials. 2020;10(4):720.
32. de Souza Furtado P, et al. In vivo evaluation of time-dependent antithrombotic effect of rivaroxaban-loaded poly(lactic-co-glycolic acid)/sodium lauryl sulfate or didodecyl dimethylammonium bromide nanoparticles in Wistar rats. Eur J Pharm Biopharm. 2023;190:184-196.